Tuning the Electrical Properties of TiO_x Bilayers Prepared by Atomic Layer Deposition at Different Temperatures

Kazuhiro Gotoh, Takeya Mochizuki, Yasuyoshi Kurokawa, Noritaka Usami*

((Optional Dedication))

Dr. K. G., Mr. T. M., Dr. Y. K., Prof. N. U.
Graduate School of Engineering, Nagoya University, Furo-Cho, Chikusa-ku, Nagoya, Aichi, 464-8603, Japan
E-mail: gotoh.kazuhiro@material.nagoya-u.ac.jp

Keywords: titanium oxide, crystalline silicon, passivation, atomic layer deposition

Carrier-selective contacts prepared by atomic layer deposition (ALD) have received significant attention for developing high-efficiency solar cells. In this work, the electrical properties of titanium oxide (TiO_x) prepared by ALD are manipulated by modulating the deposition temperature during ALD. Tunable electrical properties are possible due to the existence of oxygen vacancies in TiO_x prepared at low deposition temperature. TiO_x layers prepared at 100 °C and 150 °C provide a low contact resistivity and high passivation performance, respectively. A high carrier selectivity of 13.5 is achieved by stacking the TiO_x layers prepared at 100 °C and 150 °C, compared with a single TiO_x layer. Modulating the deposition temperature can therefore improve the electrical properties of ALD-TiO_x. This approach can be used to optimize the functionality of ALD-based materials.

1. Introduction

In recent years, crystalline silicon (c-Si) solar cells using carrier selective contacts (CSCs) have received significant attention because of their high power conversion efficiency (PCE). CSCs provide a high level of passivation performance at the c-Si surface, as well as a precise work function and band alignment against c-Si. The three factors result in efficient extraction of only one type of photo-generated carrier (i.e. electrons or holes) in c-Si. One of the most well-known types of CSC solar-cells is the Si heterojunction (SHJ) solar cell. The SHJ cell employs stacks of intrinsic hydrogenated amorphous Si (a-Si:H) and doped a-Si:H on both the front and rear side of c-Si.[1-4] However, incident photons are parasitically absorbed by doped Si-based materials[5-8], which decreases the photovoltaic power generation due to the suppression of photon absorption in c-Si.[5-7] In recent years, substantial efforts have focused on wider bandgap energy (E_g) materials for CSCs in an attempt to reduce parasitic photon absorption, and thus surpass the PCE of conventional SHJ solar cells.

One prominent material is titanium oxide (TiO_x) prepared by atomic layer deposition (ALD). ALD is a self-limited film growth method that allows for precise thickness control, uniform deposition over a large area, and little deposition damage.[9] The parasitic photon absorption of TiO_x is expected to be much lower than that of a-Si:H, since the E_g of TiO_x is 3.45 eV.[10] The ALD-TiO_x layer on c-Si can act as an electron selective contact (ESC) due to its small conduction-band offset (<0.05 eV) and large valence-band offset (>2.0 eV).[11] Thin ALD-TiO_x layers have demonstrated a high level of surface passivation on p-type and n-type c-Si surfaces after post-annealing.[12-21] In principle, CSCs with lower contact resistivity (ρ_c) are also a prerequisite for higher PCE solar cells as well as higher passivation performance. Attempts to decrease the ρ_c of ALD-TiO_x layers have been made by increasing the oxygen vacancies in the ALD-TiO_x layer during post-annealing,[13,22] and using a calcium electrode with a lower work function.[21,23]

In general, the deposition temperature of the ALD process has an impact on the chemical composition of ALD-materials.[20,24-28] Oxygen deficiencies in ALD-TiO_x are induced by a lower deposition temperature[24], whereupon oxygen vacancies act as electron donors in ALD-TiO_x, leading to higher electrical conductivity.[29,30] In this study, we focused on stacking TiO_x layers prepared at different temperatures to realize CSCs with superior electrical properties. We revealed that ALD-TiO_x single layers deposited at 100 °C and 150 °C are conductive and passivating layers, respectively. The ALD-TiO_x bilayers prepared at different temperatures show improved contact properties compared to ALD-TiO_x single layers.

2. Results and Discussion

Three kinds of ALD-TiO_x samples were prepared: (a) a TiO_x single layer deposited at 100 °C, (b) a TiO_x single layer deposited at 150 °C, and (c) stacked layers of TiO_x grown at 100 °C and 150 °C. These three samples are hereafter referred to as low temperature TiO_x (LT-TiO_x), high temperature TiO_x (HT-TiO_x), and TiO_x bilayer, respectively. Their schematic structures are illustrated in **Figure 1**. Further details are described in the Experimental Section.

Figure 2 shows XPS spectra of the Ti 2p core line for the 4-nm-thick (a) LT-TiO_x and (b) HT-TiO_x single layer after forming gas annealing (FGA). The black solid, black dashed, and red solid lines are the measured spectra, baselines, and fitted lines, respectively. The fitted lines are composed of various components shown as green lines below. The measured Ti 2p spectra of all samples show the two binding energies of the Ti $2p_{1/2}$ and Ti $2p_{3/2}$ peaks. The peak positions and the full width at half maximum (FWHM) of the Ti $2p_{3/2}$ peak are 459.0 eV and 1.16 eV for HT-TiO_x, and 458.8 eV and 1.31 eV for LT-TiO_x, respectively. The peak positions are in good agreement with reported values of ~458.8 eV for the Ti^{4+} $2p_{3/2}$ peak.[31,32] A stronger intensity of the Ti^{3+} $2p_{3/2}$ peak located at ~457.0 eV is observed in the

spectrum of LT-TiO_x, which is caused by the appearance of Ti species with a lower valence state than Ti^{4+}.[31,33] In addition, a broader FWHM is observed for the Ti $2p_{3/2}$ peaks in the spectrum of the LT-TiO_x layer, which is also associated with the presence of oxygen vacancies.[34] XPS spectra of the O 1s core line for the LT-TiO_x and HT-TiO_x single layers were investigated, however there is no noticeable difference (see Supporting Information **Figure S1**). These results suggest that the deficiency of oxygen is more pronounced in LT-TiO_x compared with HT-TiO_x. **Figure 3** shows valence band spectra of the (a) LT-TiO_x and (b) HT-TiO_x single layers as measured by ultraviolet photoelectron spectroscopy (UPS). The work functions are 3.8 eV for LT-TiO_x and 3.9 eV for HT-TiO_x. The lower work function of LT-TiO_x can be explained by the non-stoichiometric TiO_x, because the oxygen deficiency in TiO_x acts as an electron donor.[29,30] The XPS and UPS analyses indicate that the LT-TiO_x single layer is non-stoichiometric in comparison with the HT-TiO_x single layer.

Figure 4a shows the recombination current density (J_0) measured from symmetric samples of the LT-TiO_x and HT-TiO_x single layers after FGA as a function of the layer thickness. The measured J_0 of both samples decreases as the layer thickness increases from 1 nm to 4 nm. This indicates that the passivation performance increases with increasing layer thickness, in agreement with previous reports.[12,13,21,35] The passivation performance of the LT-TiO_x layers is lower than that of the HT-TiO_x layers, regardless of the layer thickness. We previously reported that the passivation mechanism of ALD-TiO_x on c-Si is related to the formation of Si-O(-Ti) bonds at the interface.[36] Therefore, the lower passivation performance of the LT-TiO_x layers is mainly attributed to insufficient oxygen in TiO_x caused by the lower deposition temperature. **Figure 4b** shows the ρ_c of the LT-TiO_x and HT-TiO_x single layers after FGA as a function of the layer thickness. To obtain the ρ_c, the Cox-Strack method was employed.[37] The ρ_c of the LT-TiO_x layers is lower than that of the HT-TiO_x layers, regardless of the layer thickness. The decrease in the ρ_c at the TiO_x/c-Si interface would be

caused by the nature of the self-formed SiO_x interlayer. Dwivedi *et al.* reported the generation of a SiO_x interlayer or a mixed oxide layer at the TiO_x/c-Si interface in the early stages of the ALD process,[38] and the chemical composition of this early-formed layer could be influenced by the TiO_x layer. Therefore, non-stoichiometric SiO_x interlayers are presumably formed at the lower deposition temperature, leading to higher conductivity. Meanwhile, oxygen vacancies induced by the lower deposition temperature during ALD act as donors, leading to higher conductivity of the TiO_x. From the J_0 and ρ_c, the contact selectivity (S_{10}), which is a figure of merit of CSCs, can be calculated by the following equation,

$$S_{10} = \log_{10}\left(\frac{V_{th}}{J_0 \rho_c}\right) \quad (1)$$

where V_{th} is the thermal voltage at 25 °C. Brendel *et al.* defined the S_{10} as a quantitative value of the potential of CSCs.[39] **Figure 4c** shows the S_{10} of the LT-TiO_x and HT-TiO_x layers as a function of the layer thickness. The S_{10} of the LT-TiO_x and HT-TiO_x layers show almost the same values and identical thickness dependencies, although both samples show different J_0 and ρ_c values due to their different chemical compositions. These results indicate that the J_0 and ρ_c values can be tuned by modulating the deposition temperature during ALD.

Next, we investigated the effect of combining the LT-TiO_x and HT-TiO_x layers, as well as the electrical properties of the resulting TiO_x bilayer. **Figure 5a**, **5b**, and **5c** show the effect of layer thickness on the J_0, ρ_c and S_{10} of the TiO_x bilayers after FGA, respectively. The J_0 decreases with increasing thickness of the HT-TiO_x layer. The highest and lowest J_0 values of 68.0 fA/cm^2 and 33.6 fA/cm^2 are obtained from the single LT-TiO_x layer and single HT-TiO_x layer, respectively. The higher passivation performance with thicker HT-TiO_x layers is attributed to the effective formation of Si-O bonds at the TiO_x/c-Si interface.[35,36] Furthermore, the decrease in J_0 values is less pronounced when the thickness of the HT-TiO_x layer exceeds 2 nm. The small decreasing rate of J_0 is possibly due to insufficient oxygen in

LT-TiO_x. The ρ_c increases linearly with increasing HT-TiO_x layer thickness. Therefore, the reduction of ρ_c is possibly due to the trap-assisted carrier transport via oxygen vacancies in the LT-TiO_x layers. In this structure, the passivation performance is dominated by the 2-nm-thick HT-TiO_x, since the chemical composition of self-formed SiO_x at the TiO_x/c-Si interface depends on the initially deposited HT-TiO_x layers on c-Si. Consequently, the TiO_x stacks with 2-nm- or 3-nm-thick HT-TiO_x layers show slightly higher S_{10} values than the other samples, resulting from the trade-off relationship between ρ_c and J_0. The highest value of S_{10} is 13.5, which is higher than that obtained from TiO_x-based CSCs used in high performance SHJ solar cells.[19] These results indicate that changing the deposition temperature (T_{depo}) during the ALD process can improve the electrical properties of TiO_x layers.

3. Conclusion

We have demonstrated that TiO_x bilayers consisting of HT-TiO_x and LT-TiO_x layers obtained by changing the T_{depo} during ALD can realize high passivation performance and a low ρ_c on c-Si. XPS analysis revealed that more oxygen vacancies are present in the LT-TiO_x layers compared with the HT-TiO_x layers. The work function of the LT-TiO_x single layer is smaller than that of the HT-TiO_x single layer, possibly due to the oxygen vacancies. Hence, the HT-TiO_x and LT-TiO_x layers act as an excellent passivating layer and conductive layer, respectively. The trade-off relationship between J_0 and ρ_c occurs in the ALD-TiO_x single layer. The bilayer consisting of the LT-TiO_x and HT-TiO_x layers exhibits superior electrical properties compared with the ALD-TiO_x single layer. The bilayer is therefore promising for optimizing the electrical properties of ALD-based materials.

4. Experimental Section

All experiments were performed using double-side mirror-polished float-zone (FZ) grown n-type c-Si(100) wafers. The resistivity and thickness were 2.0–5.0 Ω·cm and ~280

μm, respectively. Prior to deposition of the TiO_x thin layer, c-Si wafers were dipped in 5% hydrofluoric acid for 30 sec to remove the native silicon oxide. TiO_x layers were deposited by thermal ALD (GEMStar-6, Arradiance). In the ALD process, tetrakis-dimethyl-amido titanium (TDMAT), H_2O and N_2 (99.999%) were used as the titanium precursor, oxidant, and purging gas, respectively. Two different T_{depo} of 100 °C and 150 °C were employed to deposit ALD-TiO_x. We fabricated three kinds of TiO_x samples: (a) a TiO_x single layer deposited at 100 °C (LT-TiO_x), (b) a TiO_x single layer deposited at 150 °C (HT-TiO_x), and (c) a stack of HT-TiO_x and LT-TiO_x (see **Figure 1**). For fabrication of the TiO_x bilayers, the HT-TiO_x layers were deposited on c-Si, and the LT-TiO_x layers were subsequently deposited without exposure to air (see Supporting Information **Figure S2**). After the deposition of ALD-TiO_x, FGA at 350 °C for 3 min was carried out in a mixed gas (3% H_2 and 97% Ar), which yielded a relatively high passivation performance for the ALD-TiO_x/c-Si[39] and ALD-TiO_x/SiO_x/c-Si structures.[36]

The layer thickness was measured by a spectroscopic ellipsometer (SE) (M-2000DI, J. A. Woollam). In SE analysis, the Tauc-Lorentz model was used for the ALD-TiO_x layers. To investigate the chemical bonding features in the region near the TiO_x/c-Si interface, XPS measurements under monochromatized Al K_α X-ray radiation ($h\nu$ = 1486.6 eV) were performed at a photoelectron take-off angle of 30° and a measurement energy step of 0.05 eV. The work functions of the LT-TiO_x and HT-TiO_x single layers were measured by UPS. The excitation source for the UPS measurements was He I (21.22 eV). The samples were placed under an applied bias of –10 V during the UPS measurements. The Fermi energy was determined by comparison to a gold reference. The work functions were determined by subtracting the energy width of the UPS spectrum from the energy of the excitation source. For all samples, the J_0 and ρ_c were measured to assess their potential as an ESC. The J_0 values of symmetric structures on c-Si before metallization were derived from the

measurement with a WCT-120TS lifetime tester (Sinton Instrument) at room temperature. For measuring the ρ_c by the Cox-Strack method[38], the TiO_x layers were prepared on the front side of n-type c-Si. On the rear side, a full-area antimony-doped gold contact of 80 nm in thickness was evaporated. On the TiO_x side, six aluminum dots of 80 nm in thickness with different diameters ranging from 0.2 mm to 1.0 mm were deposited by thermal evaporation using a shadow mask. The ρ_c was extracted from the fitting of resistance versus the dot diameter (see Supporting Information **Figure S3**). The values of resistance were calculated from the results of *I-V* measurements for each aluminum dot.

Acknowledgements

This work was supported by the New Energy and Industrial Technology Development Organization (NEDO) in Japan. We thank H. Miura and A. Shimizu for their technical support. We also thank Dr. Mel F. Hainey Jr. for helpful discussion during the preparation of this manuscript, N. Saito, M. A. Bratescu, J. Hieda and K. Yamamoto for their help with XPS measurements, and Aidan G. Young, PhD, from Edanz Group (www.edanzediting.com/ac) for editing a draft of this manuscript.

Received: ((will be filled in by the editorial staff))
Revised: ((will be filled in by the editorial staff))
Published online: ((will be filled in by the editorial staff))

References

[1] M. Taguchi, A. Yano, S. Tohoba, K. Matsuyama, Y. Nakamura, T. Nishikawa, K. Fujita, E. Maruyama, *IEEE J. Photovoltaics* **2014**, *4*, 95.

[2] D. Adachi, J. L. Hernandez, K. Yamamoto, *Appl. Phys. Lett.* **2015**, *107*, 233506.

[3] K. Yoshikawa, H. Kawasaki, W. Yoshida, K. Konishi, K. Nakano, T. Uno, D. Adachi, M. Kanematsu, H. Uzu, K. Yamamoto, *Nat. Energy* **2017**, *2*, 17032.

[4] C. Battaglia, A. Cuevas, S. De Wolf, *Energy Environ. Sci.* **2016**, *9*, 1552.

[5] A. A. Langford, M. L. Fleet, B. P. Nelson, *Phys. Rev. B* **1992**, *45*, 23.

[6] A. S. Ferlauto, G. M. Ferreira, J. M. Pearce, C. R. Wronski, R. W. Collins, X. Deng, G. Ganguly, *J. Appl. Phys.* **2002**, *92*, 5.

[7] Z. C. Holman, A. Descoeudres, L. Barraud, F. Z. Fernandez, J. P. Seif, S. De Wolf, C. Ballif, *IEEE J. Photovoltaics* **2012**, *2*, 7.

[8] M. Rienacker, M. Bossmeyer, A. Merkle, U. Höhne, F. Haase, J. Krugener, R. Brendel, R. Peibst, *IEEE J. Photovoltaics* **2017**, ***7***, 11.

[9] R. L. Puurunen, *J. Appl. Phys.* **2005**, *97*, 121301.

[10] J. Bullock, Y. Wan, Z. Xu, S. Essig, M. Hettick, H. Wang, W. Ji, M. Boccard, A. Cuevas, C. Ballif, A. Javey, *ACS Energy Lett.* **2018**, *3*, 508.

[11] S. Avasthi, W. E. McClain, G. Man, A. Kahn, J. Schwar, J. C. Strum, *Appl. Phys, Lett.* **2013**, *102*, 203901.

[12] X. Yang, P. Zheng, Q. Bi, K. Weber, *Sol. Energy Mater. Sol. Cells* **2016**, *150*, 32.

[13] X. Yang, Q. Bi, H. Ali, K. Davis, W. V. Schoenfeld, K. Weber, *Adv. Mater.* **2016**, *28*, 5891.

[14] B. Liao, B. Hoex, A. G. Aberle, D. Chi, C. S. Bhatia, *Appl. Phys. Lett.* **2014**, *104*, 253903.

[15] B. Liao, B. Hoex, K. D. Shetty, P. K. Basu, C. S. Bhatia, *IEEE J. Photovoltaics* **2015**, *5*, 1062.

[16] K. M. Gad, D. Vossing, A. Richter, B. Rayner, L. M. Reindl, S. E. Mohney, M. Kasemann, *IEEE J. Photovoltaics* **2016**, *6*, 649.

[17] M. M. Plakhotnyuk, N. Schuler, E. Shkodin, R. A. Vijayan, S. Masilamani, M. Varadharajaperumal, A. Crovetto, O. Hansen, *Jpn. J. Appl. Phys.* **2017**, *56*, 1.

[18] V. Titova, B. V.-Wolf, D. Startsev, J. Schmidt, *Energy Procedia* **2017**, *124*, 441.

[19] X. Yang, K. Weber, Z. Hameiri, S. D. Wolf, *Prog. Photovoltaics Res. Appl.* **2017**, *25*, 896.

[20] T.-C. Chen, T.-C. Yang, H.-E. Cheng, I.-S. Yu, Z.-P. Yang, *Appl. Surf. Sci.* **2018**, *451*, 121.

[21] T. G. Allen, J. Bullock, Q. Jeangros, C. Samundsett, Y. Wan, J. Cui, A. H.-Wyser, S. De Wolf, A. Javey, A. Cuevas, *Avd. Energy Mater.* **2017**, *12*, 1602606.

[22] H. Ali, X. Yang, K. Weber, W. V. Schoenfeld, K. O. Davis, *Microsc. Microanal.* **2017**, *23*, 900.

[23] J. Cho, J. Melskens, M. Debucquoy, M. R. Payo, S. Jambaldinni, T. Bearda, I. Gordon, J. Szlufcik, W. M. M. Kessels, J. Poortmans, *Prog. Photovoltaics Res. Appl.* **2018**, *26*, 835.

[24] J. Aarik, A. Aidla, A. Kiisler, T. Uustare, V. Sammelselg, *Thin Solid Films* **1997**, *305*, 270.

[25] S. B. Basuvalingam, B. Macco, H. C. M. Knoops, J. Melskens, W. M. M. Kessels, A. A. Bol, *J. Vac. Sci. Technol. A* **2018**, *36*, 041503.

[26] M. Mattinen, P. J. King, L. Khriachtchev, M. J. Heikkiä, B. Fleming, S. Rushworth, K. Mizohata, K. Meinander, J. Räisänen, M. Ritala, M. Leskelä, *Mater. Today Chem.* **2018**, *9*, 17.

[27] M. Mattinen, J.-L. Wree, N. Stegmann, E. Ciftyurek, M. E. Achhad, P. J. King, K. Mizohata, J. Räisänen, K. D. Schierbaum, A. Devi, M. Ritala, M. Leskelä, *Chem. Mater.* **2018**, *30*, 8690.

[28] A. Sharma, V. Longo, M. A. Verheijen, A. A. Bol, W. M. M. Kessels, *J. Vac. Sci. Technol. A* **2018**, *35*, 01B130.

[29] A. Agrawal, J. Lin, M. Barth, R. White, B. Zheng, S. Chopra, S. Gupta, K. Wang, J. Gelatos, S. E. Mohney, S. Datta, *Appl. Phys. Lett.* **2014**, *104*, 112101.

[30] M. T. Greiner, M. G. Helander, W.-M. Tang, Z.-B. Wang, J. Qiu, Z.-H. Lu, *Nat. Mater.* **2011**, *11*, 76.

[31] Y. Fu, H. Du, S. Zhang, W. Huang, *Mater. Sci. Eng.* **2005**, *403*, 25.

[32] U. Diebold, *Surf. Sci. Rep.* **2003**, *48*, 53.

[33] W. Gopel, J. A. Anderson, D. Frankel, M. Jaehing, K. Phillips, J. A. Schfer, G. Rocker, *Surf. Sci.* **1984**, *139*, 333.

[34] K. V. Egorov, D. S. Kuzmichev, Y. Y. Lebedinskii, C. S. Hwang, A. M. Markeev, *ACS Appl. Mater. Interfaces* **2017**, *9*, 13286.

[35] T. Mochizuki, K. Gotoh, Y. Kurokawa, T. Yamamoto, N. Usami, *Adv. Mater. Interfaces* **2018**, *5*, 1801645.

[36] T. Mochizuki, K. Gotoh, A. Ohta, S. Ogura, Y. Kurokawa, S. Miyazaki, K. Fukutani, N. Usami, *Appl. Phys. Express* **2018**, *11*, 102301.

[37] R. Cox, H. Strack, *Solid-State Electron.* **1967**, *10*, 1213.

[38] N. Dwivedi, R. J. Yeo, H. R. Tan, R. Stangl, A. G. Aberle, C. S. Bhatia, A. Danner, B. Liao, *Adv. Funct. Mater.* **2018**, *28*, 1707018.

[39] R. Brendel, R. Peidst, *IEEE J. Photovoltaics* **2016**, *6*, 1413.

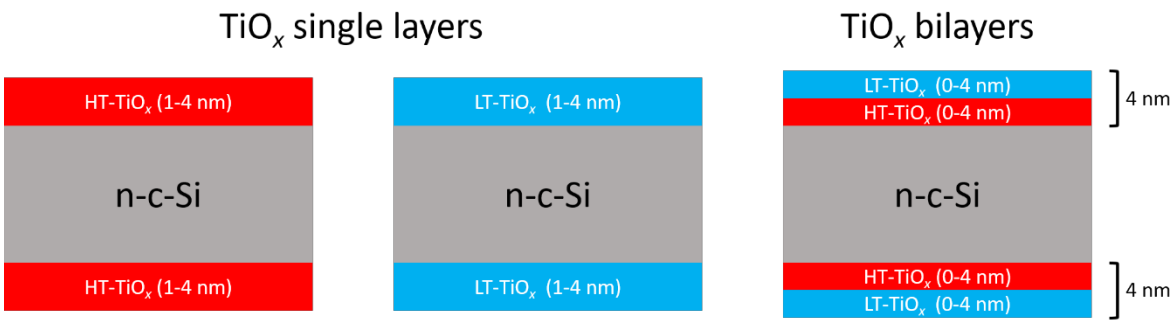

Figure 1. Cross-sectional schematics of the fabricated ALD-TiO_x structures. HT-TiO_x and LT-TiO_x represent TiO_x single layers deposited at 150 °C and 100 °C, respectively. For TiO_x single layers, the thickness is in the range of 1–4 nm. For TiO_x bilayers, the total thickness is fixed at 4 nm.

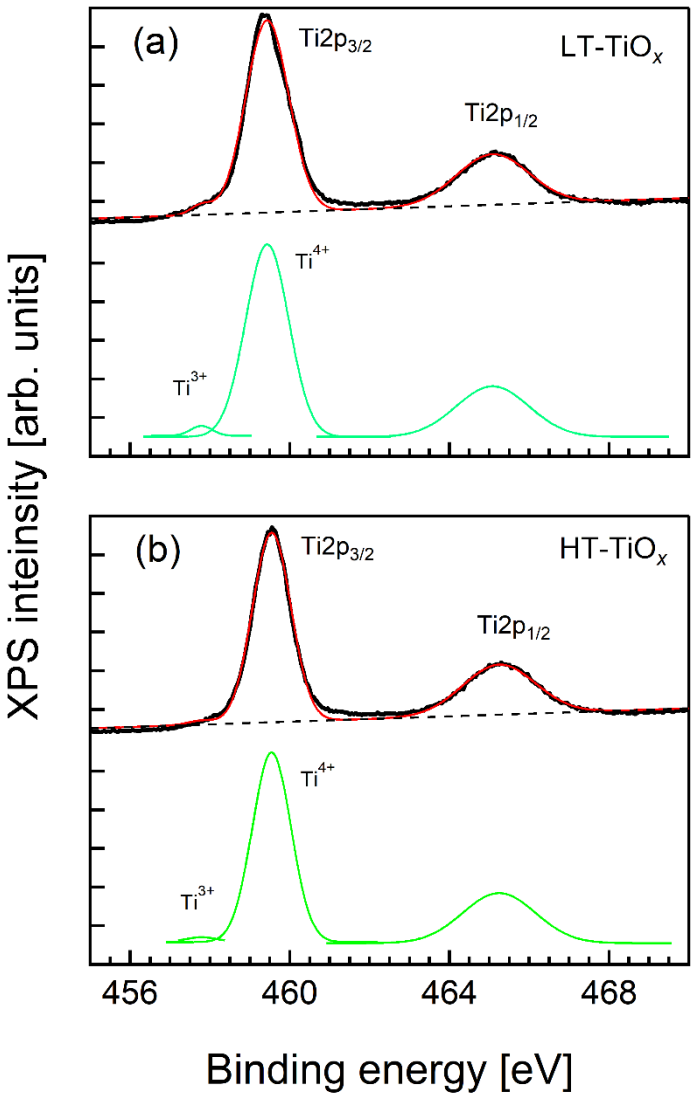

Figure 2. XPS spectra of the Ti 2p core line for annealed TiO_x single layers formed at (a) 100 °C (LT-TiO_x) and (b) 150 °C (HT-TiO_x). Black solid, black dashed, red solid, and green solid lines are the measured spectra, baseline, cumulated fitted and individual fitted lines, respectively.

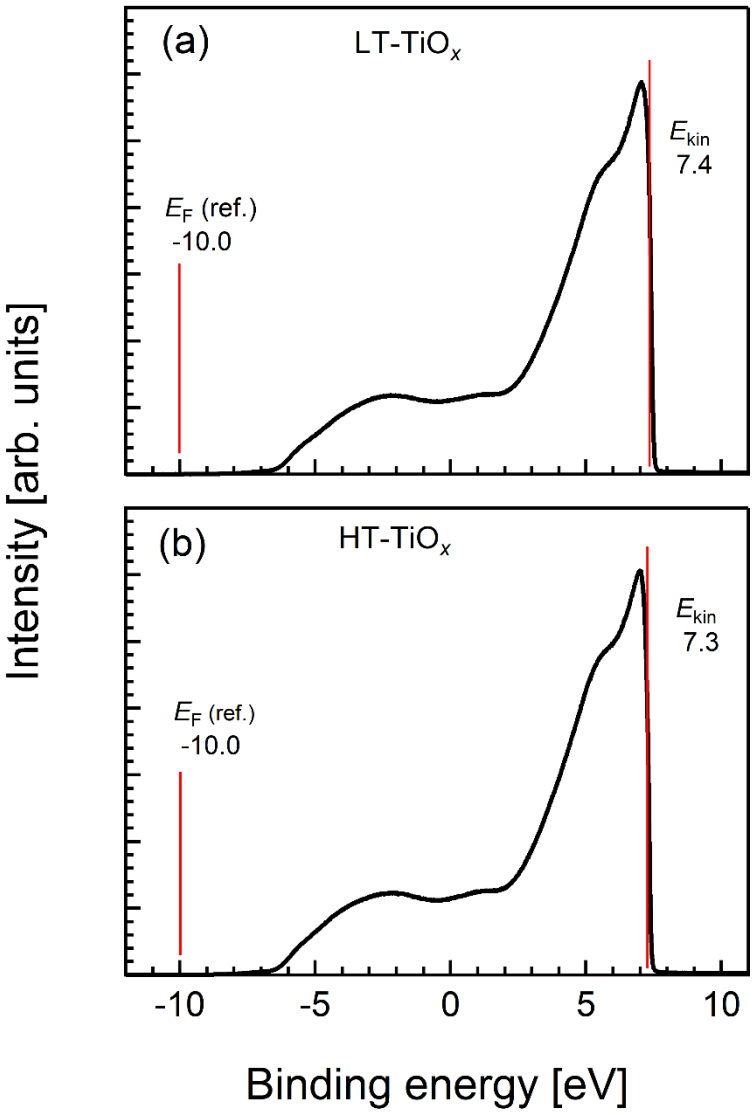

Figure 3. Valence band spectra of annealed TiO_x single layers prepared at (a) 100 °C (LT-TiO_x) and (b) 150 °C (HT-TiO_x). The measurements were carried out under –10 V. The Fermi energy E_F was determined by comparison to a gold reference. The work function was determined by subtracting the energy width of the UPS spectrum ($E_{kin} - E_F$) from the energy of the excitation source.

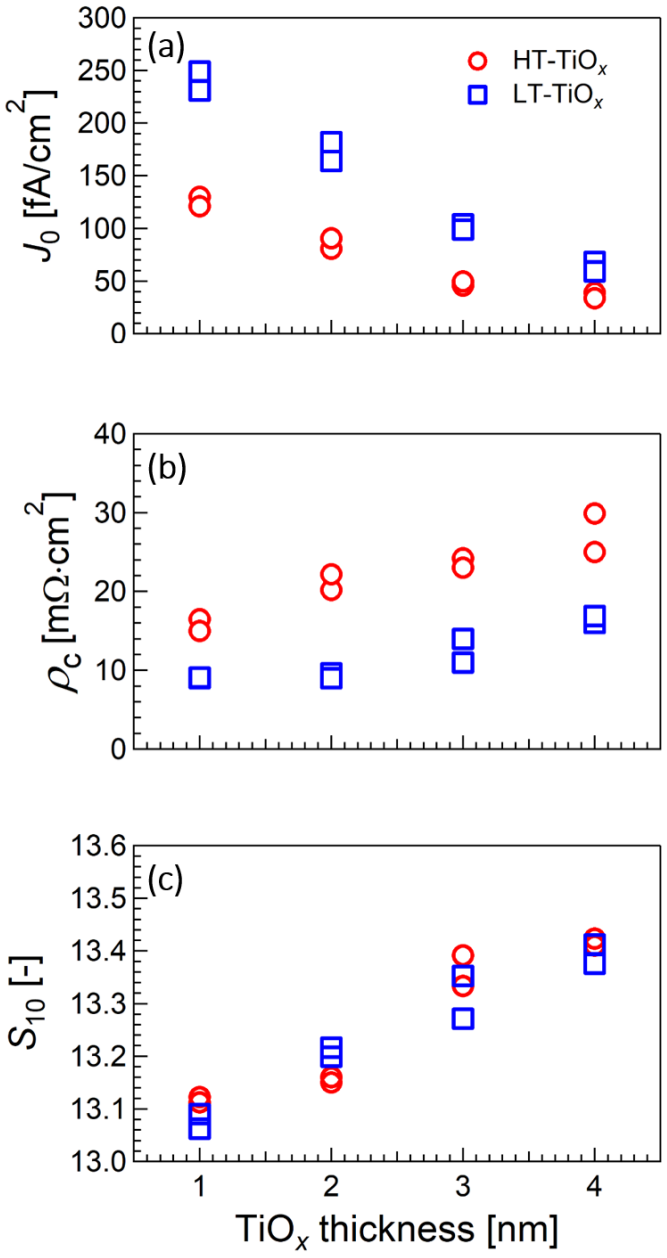

Figure 4. Effect of layer thickness of annealed TiO_x single layers on the (a) recombination current density, (b) contact resistivity and (c) carrier selectivity. HT-TiO_x and LT-TiO_x are represented by open circles and squares, respectively.

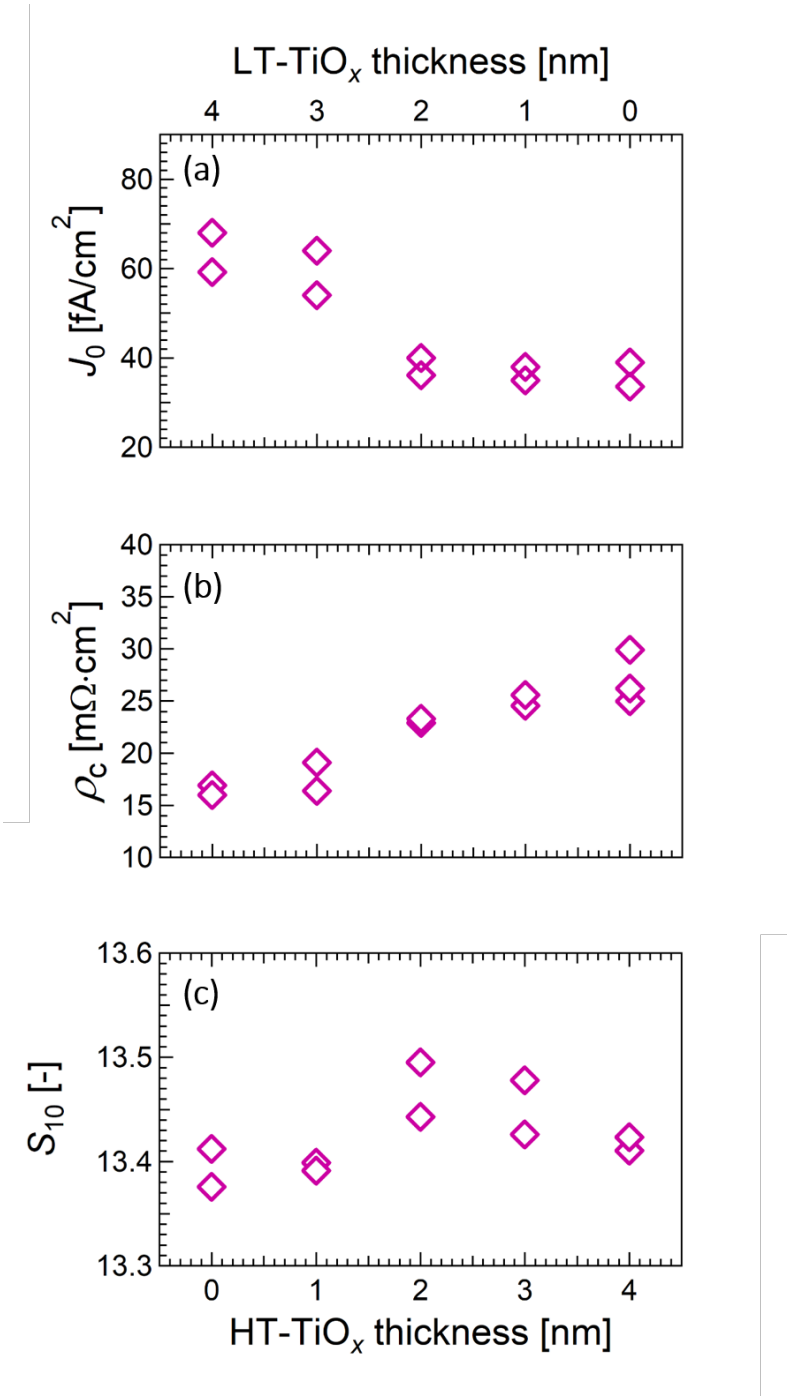

Figure 5. (a) Recombination current density, (b) contact resistivity and (c) carrier selectivity of annealed TiO_x bilayers as a function of the LT-TiO_x and HT-TiO_x thicknesses.

The table of contents entry

Tuning of the electrical properties of TiO_x/Si heterostructures prepared by atomic layer deposition is demonstrated using TiO_x bilayers. The TiO_x bilayer exhibits superior electrical properties to TiO_x single layers. The tunable electrical properties are attributed to oxygen vacancies in the TiO_x films. The fabrication process can be applied to various ALD-based materials.

Keyword titanium oxide, crystalline silicon, passivation, atomic layer deposition

K. Gotoh*, T. Mochizuki, Y. Kurokawa, N. Usami

Tuning the Electrical Properties of TiO_x Bilayers Prepared by Atomic Layer Deposition at Different Temperatures

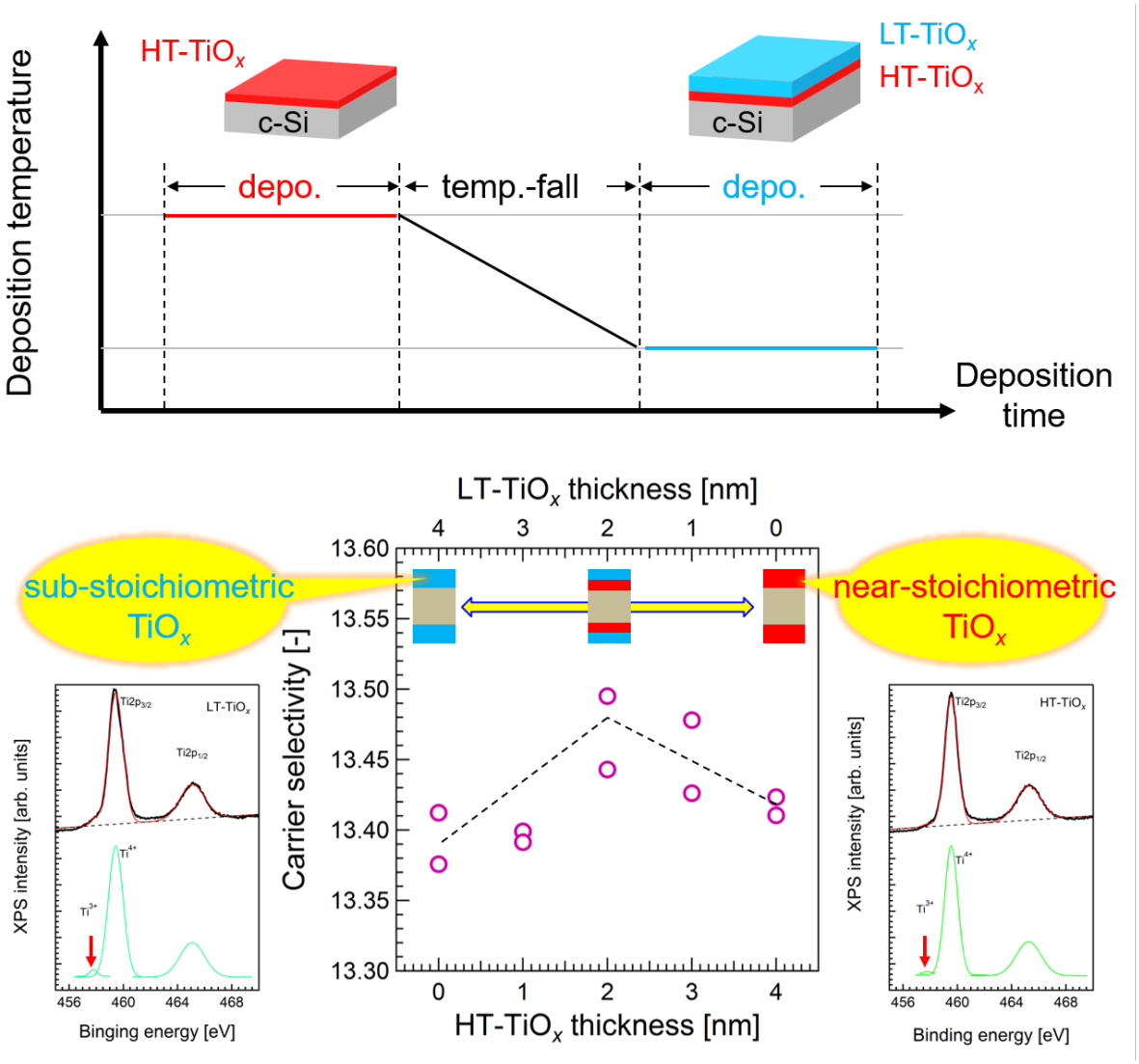

Supporting Information

Tuning the Electrical Properties of TiO_x Bilayers Prepared by Atomic Layer Deposition at Different Temperatures

Kazuhiro Gotoh, Takeya Mochizuki, Yasuyoshi Kurokawa, Noritaka Usami*

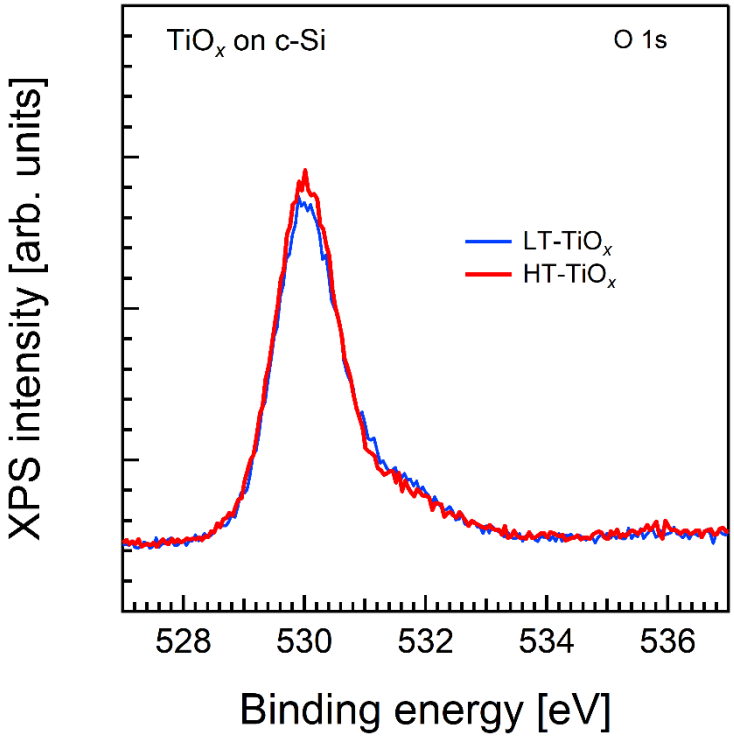

Figure S1. XPS spectra of the O 1s core line for annealed TiO_x single layers formed at (a) 100 °C (LT-TiO_x) and (b) 150 °C (HT-TiO_x).

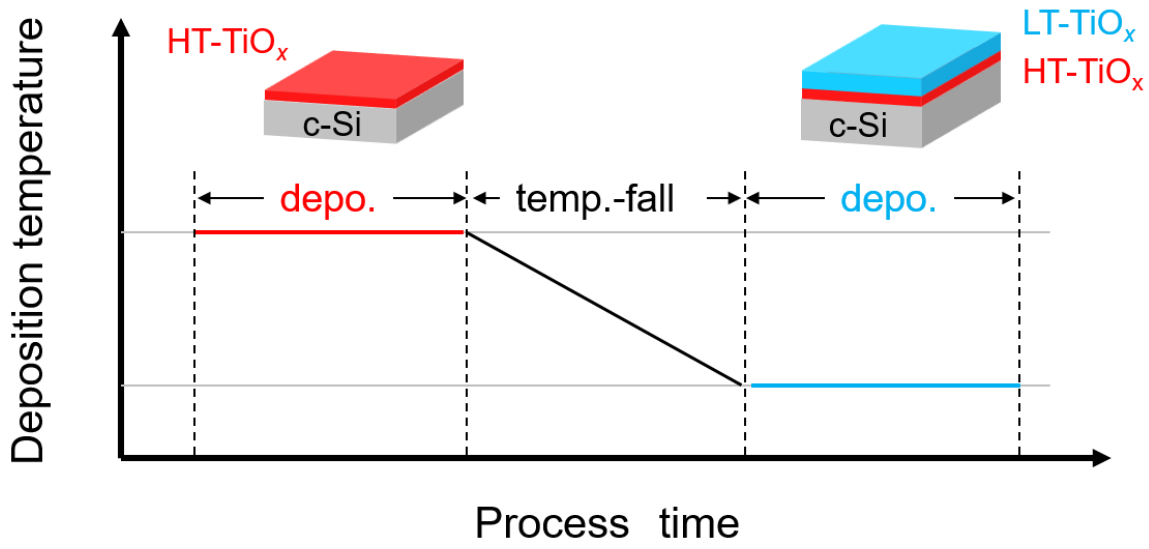

Figure S2. Schematic deposition process of ALD-TiO_x bilayers. HT-TiO_x and LT-TiO_x represent ALD-TiO_x single layers prepared at high and low temperature, respectively.

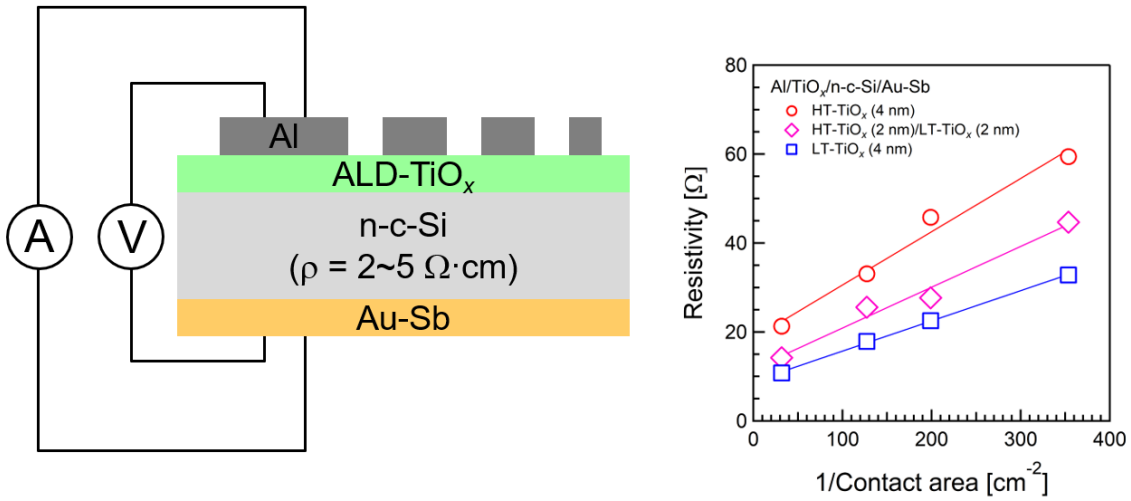

Figure S3. (Left) Schematic sample structure for the Cox-Strack method. (Right) Extraction of contact resistivity of Al/TiO_x on n-c-Si via fitting a series of current verses voltage measurements.